# Dalton Transactions

## Accepted Manuscript

This article can be cited before page numbers have been issued, to do this please use: A. Schejn, T. Mazet, V. falk, B. Lavinia, L. aranda, G. medjahdi and R. Schneider, *Dalton Trans.*, 2015, DOI: 10.1039/C5DT01191D.




ROYAL SOCIETY OF CHEMISTRY

www.rsc.org/dalton

Dalton Transactions

Dynamic Article Links ►
View Article Online
DOI: 10.1039/C5DT01191D

Cite this: DOI: 10.1039/c0xx00000x

www.rsc.org/xxxxxx

ARTICLE TYPE

# $Fe_3O_4$@ZIF-8: Magnetically recoverable catalysts by loading $Fe_3O_4$ nanoparticles inside a zinc imidazolate framework

**Aleksandra Schejn,[a] Thomas Mazet,[b] Véronique Falk,[a] Lavinia Balan,[c] Lionel Aranda,[b] Ghouti Medjahdi[b] and Raphaël Schneider*[a]**

***Received (in XXX, XXX) Xth XXXXXXXXX 20XX, Accepted Xth XXXXXXXXX 20XX***
**DOI: 10.1039/b000000x**

**A simple methodology for encapsulating ca. 10 nm-sized superparamagnetic $Fe_3O_4$ nanoparticles in zeolitic imidazolate frameworks (ZIF-8) crystals was developed. The corresponding $Fe_3O_4$@ZIF-8 heterostructured material exhibits bifunctional properties with both high magnetization ($Fe_3O_4$) and high thermal stability, large specific surface, and catalytic properties (ZIF-8). The $Fe_3O_4$@ZIF-8 catalyst exhibits fair separation ability and reusability, which can be repeatedly applied for Knoevenagel condensations and Huisgen cycloadditions for at least ten successive cycles.**

Among metal organic frameworks (MOFs), zeolitic imidazolate frameworks (ZIFs) are microporous crystalline materials with high thermal and chemical stability which have attracted particular attention for gas storage and gas separation.[1-4] In ZIF-8 crystals, the network consists of $Zn^{2+}$ atoms arranged as of [ZnN4] tetrahedrons with the N atoms of 2-methylimidazolate ($mim^-$) linkers.[5-8] ZIF-8 has a sodalite zeolite-type topology with cages of 11.6 Å and pores of 3.4 Å in diameter. The efficiency of ZIF-8 has been demonstrated in gas separation, gas storage, but also for heterogeneous catalytic transformations (Knoevenagel condensations, cycloadditions, oxidations, trans-esterification, and Friedel-Crafts alkylations).[8,9]

Nevertheless, one major problem with the reuse of ZIF-8 heterogeneous catalysts remains their separation from the reaction products. Because of the ease of magnetic separation from the reaction mixture, this strategy is more effective than nanofiltration through a membrane or centrifugation in that it allows the catalyst to be recovered.[10] Superparamagnetic particles are intrinsically nonmagnetic but can be readily magnetized in the presence of an external magnetic field. This property enables trouble-free separation of the particles from the reaction medium by simply applying an external magnet, thus eliminating filtration or centrifugation operations. Additionally, magnetic particles exhibit high chemical stability and can be considered as inert in most chemical transformations. Finally, magnetic separation of nanoparticles is economical and promising for industrial applications.[11-13]

In recent years, a couple of approaches have been developed for the encapsulation of small-sized functional nanoparticles like metal particles (Au, Ag, Pt, Pd, Ni)[14-28] or quantum dots (CdSe, ZnO, GaN)[29-33] into MOFs to build hybrid materials for catalytic or optical applications.[34] $Fe_3O_4$ nanoparticles capped with the [($\eta^5$-semiquinone)$Mn(CO)_3$] ligand or with polyacrylic acid have successfully been incorporated in organometallic coordination polymers involving $Mn^{2+}$, $Cd^{2+}$ or $In^{3+}$.[35,36] The MIL-100 MOF ($Fe^{3+}$ associated to 1,3,5-benzenetricarboxylate) has recently been grown onto large $Fe_3O_4$ or $Fe_3O_4$/Au particles (200-600 nm) to develop reusable catalysts for Claisen-Schmidt condensations and for the reduction of 4-nitrophenol.[37,38] A similar approach was also used to deposit small-sized ZIF-8 crystals (70-140 nm) at the outer-surface of $Fe_3O_4$ crystals (380-600 nm) to prepare core/shell $Fe_3O_4$/ZIF-8 particles without alteration of the properties of both materials.[39,40] The magnetic properties of these core/shell particles were successfully used for the deposition of catalytically active ZIF-8 material in microreactors or for the development of reusable sorbent particles.

Herein, we report for the first time a simple strategy to spread ca. 10 nm-sized $Fe_3O_4$ nanoparticles into the cavities and/or channels of ZIF-8 crystals. The porous crystalline $Fe_3O_4$@ZIF-8 particles exhibit high catalytic activity in Knoevenagel condensations and present the advantage of being magnetically recoverable at the end of reactions and reuseable for up to ten cycles with no visible deterioration of their catalytic activity. The method was successfully extended to $Cu^{2+}$-doped ZIF-8 and allowed the preparation of recyclable catalysts for Huisgen 1,3-dipolar cycloadditions.

The preparation procedure of $Fe_3O_4$@ZIF-8 particles is schematically illustrated in Fig. 1.

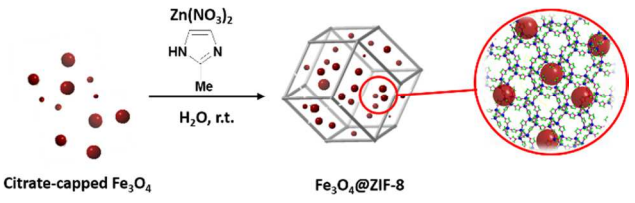


**Fig. 1** Schematic illustration of $Fe_3O_4$@ZIF-8 particles synthesis.

In order to fill up the ZIF-8 framework with $Fe_3O_4$ particles, water-dispersible $Fe_3O_4$ particles capped with citrate ligands were used.[41] The three carboxylate groups of citrate are meant to coordinate the $Zn^{2+}$ ions and once these ions react with Hmim, the ZIF-8 structure will develop around the $Fe_3O_4$ particles. In a typical synthetic procedure, citrate-capped $Fe_3O_4$ nanoparticles

View Article Online
DOI: 10.1039/C5DT01191D



and Hmim were

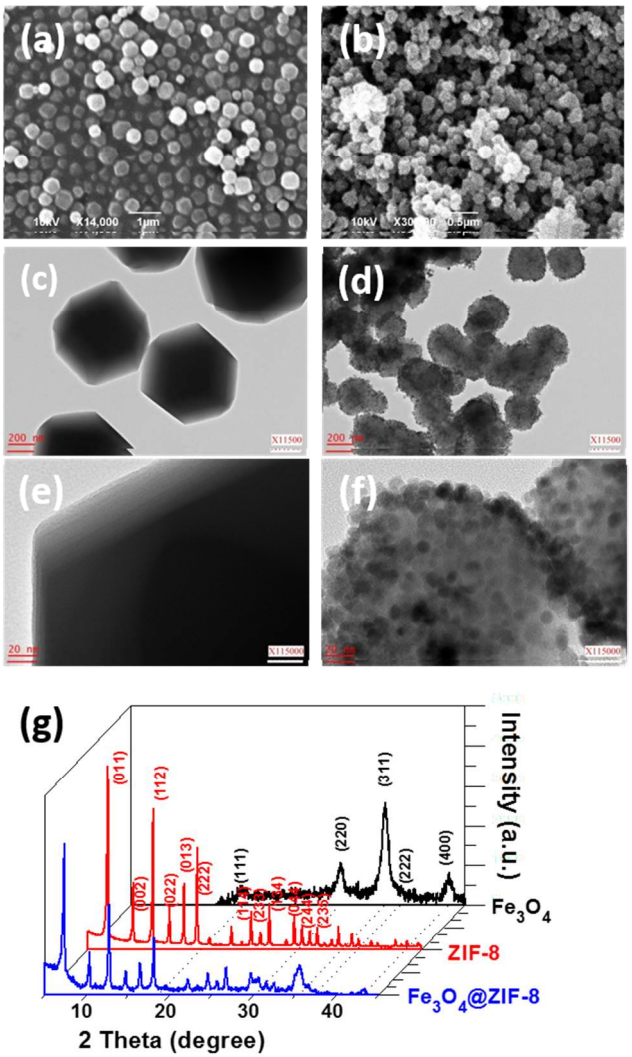


**Fig. 2** SEM images of (a) ZIF-8 and (b) $Fe_3O_4$@ZIF-8 particles. TEM pictures of (b) and (e) ZIF-8, (d) and (f) $Fe_3O_4$@ZIF-8 particles. (g) Powder XRD patterns of $Fe_3O_4$, ZIF-8, and $Fe_3O_4$@ZIF-8 crystals.

dispersed in water and the mixture stirred for 5 min under inert atmosphere. Next, an aqueous solution of $Zn(NO_3)_2$ (molar ratio Hmim/$Zn(NO_3)_2$ = 70/1) was added and the resulting mixture was stirred at room temperature for 10 min. $Fe_3O_4$@ZIF-8 crystals were separated by using an external magnetic field and purified by washing with water and ethanol. The structure and morphology of $Fe_3O_4$@ZIF-8 particles were characterized by powder X-ray diffraction (PXRD), scanning electron microscopy (SEM), transmission electron microscopy (TEM), and $N_2$ adsorption at 77K.

As shown by TEM and SEM experiments, ZIF-8 crystals exhibit the well-defined and thermodynamically favorable truncated rhombic dodecahedral shape and have an average diameter of ca. 430 nm (Fig. 2a,c,e). Once $Fe_3O_4$ nanoparticles incorporated into the ZIF-8 framework, the morphology of ZIF-8 crystals is not markedly altered but the particle size decreases to ca. 250 nm (Fig. 2b,d,f and Fig. S1 for size distributions), indicating that $Fe_3O_4$ nanoparticles act as size-controlling agents for ZIF-8 crystals. It is also worth mentioning that there is no apparent change in the diameter of $Fe_3O_4$ particles in $Fe_3O_4$@ZIF-8 compared to the

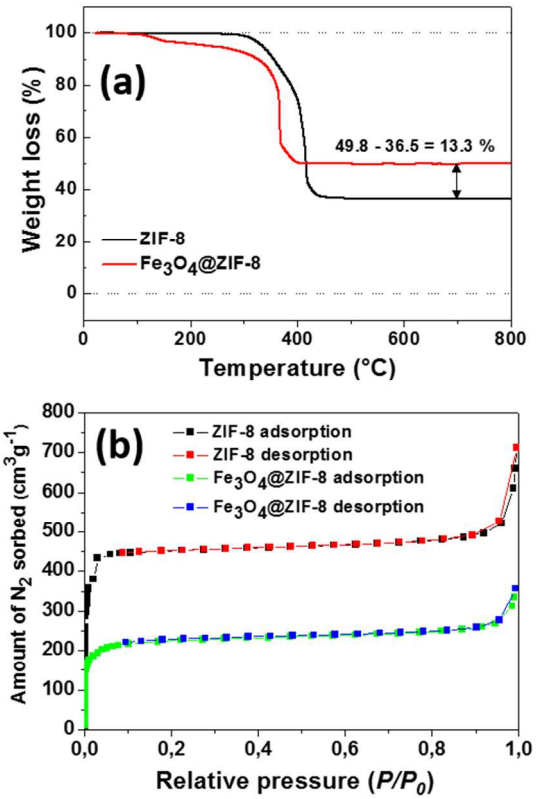


**Fig. 3** (a) TGA traces of ZIF-8 and $Fe_3O_4$@ZIF-8 crystals. (b) $N_2$ adsorption/desorption curves at 77K for ZIF-8 and $Fe_3O_4$@ZIF-8 particles giving surface areas of 1856 and 871 $m^2\ g^{-1}$, respectively. Black (green) and red (blue) data correspond to the adsorption and desorption branches, respectively.

native citrate-capped $Fe_3O_4$ particles (9.6 ± 1.9 nm) (Fig. S2).

The encapsulation of $Fe_3O_4$ in ZIF-8 was further demonstrated by powder X-ray diffraction (PXRD) analysis (Fig. 2g). $Fe_3O_4$@ZIF-8 particles exhibit a similar XRD pattern compared to ZIF-8 indicating that the sodalite structure of ZIF-8 crystals remained unaffected after loading the $Fe_3O_4$ particles.[5,8] Except three peaks at 2Θ = 48.75, 50.37, and 57.22°, which correspond to the (220), (311), and (400) crystal facets of magnetite (JCPDS No 19-0629), no additional peaks were detected indicating the high purity of the final $Fe_3O_4$@ZIF-8 particles.

Thermogravimetric analysis (TGA) conducted under air indicate that $Fe_3O_4$@ZIF-8 particles have a slightly lower stability than ZIF-8 crystals (Fig. 3a). For ZIF-8, the sharp weight loss step of 63-64% was observed at ca. 400°C, corresponding to the decomposition of the $mim^-$ linker and to the formation of ZnO crystals.[8] The relatively lower decomposition temperature of $Fe_3O_4$@ZIF-8 (350°C) compared to pure ZIF-8 might be attributed to the gradual decomposition of the citrate ligand capping $Fe_3O_4$ nanoparticles into aconitate and citraconate between 150 and 350°C. Finally, when comparing the weight loss of ZIF-8 and $Fe_3O_4$@ZIF-8 particles, the loading of $Fe_3O_4$ into ZIF-8 host was estimated to be 13.3%.

View Article Online
DOI: 10.1039/C5DT01191D



Textural parameters such as surface area, pore volume and pore size of $Fe_3O_4$@ZIF-8 particles were obtained from $N_2$ adsorption-desorption measurements at 77K. As shown in Fig. 3b, both ZIF-8 and $Fe_3O_4$@ZIF-8 particles display the Type I isotherms, with a

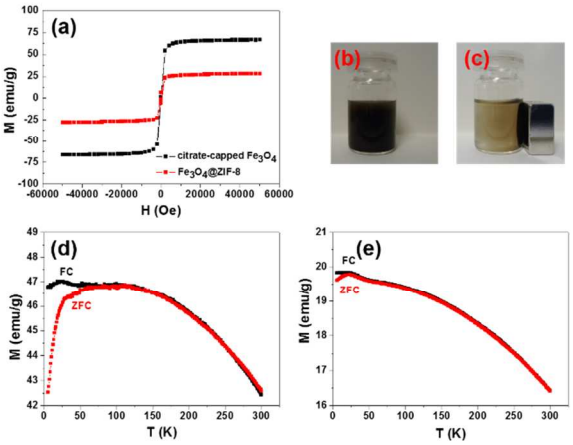


**Fig. 4** (a) Magnetization at 300 K as a function of applied field. Optical images of $Fe_3O_4$@ZIF-8 particles dispersions (b) before and (c) after applying an external magnetic field. (d,e) Temperature dependent magnetization for citrate-capped $Fe_3O_4$ and $Fe_3O_4$@ZIF-8 particles, respectively.

steep increase for the $N_2$ uptake at low relative pressure, which reveals the microporosity for both types of particles. The specific surface areas, determined using the Brunauer-Emmet-Teller (BET) method, were found to be 871 ± 3 and 1856 ± 46 $m^2/g$ for $Fe_3O_4$@ZIF-8 and ZIF-8 particles, respectively. The pore volume was also found to decrease from 0.71 $cm^3/g$ for ZIF-8 to 0.35 $cm^3/g$ for $Fe_3O_4$@ZIF-8. The high decrease in surface area and pore volume after loading $Fe_3O_4$ nanoparticles into ZIF-8 are not surprising since $Fe_3O_4$ particles are nonporous. These results also indicate that the cavities of ZIF-8 framework are blocked by the highly dispersed $Fe_3O_4$ nanoparticles which seem to be mainly located at the surface of ZIF-8 crystals as indicated by TEM images (Fig. 2d,f).

The temperature dependence of the magnetization recorded in FC and ZFC conditions (H = 1000 Oe) exhibits characteristic features of superparamagnetism for both $Fe_3O_4$ and $Fe_3O_4$@ZIF-8 crystals (Fig. 4): (i) the ZFC curves go to a rounded maximum at the blocking temperature TB ~ 55 K and ~ 25 K for $Fe_3O_4$ and $Fe_3O_4$@ZIF-8, respectively and (ii) the room-temperature hysteresis loop points to negligible coercivity and remanence. The lower blocking temperature of $Fe_3O_4$@ZIF-8 compared to citrate-capped $Fe_3O_4$ particles originates from reduced dipolar interactions between magnetic particles encapsulated in ZIF-8 pores.[42,43] The significantly broader peak observed for $Fe_3O_4$ implies a distribution of blocking temperature. Since the particle size does not significantly differ for the two materials, the distribution of TB in $Fe_3O_4$ is likely due to variation in interparticle interactions across the sample.

To compare the catalytic properties of $Fe_3O_4$@ZIF-8 with those of pure ZIF-8 crystals, we first evaluated their catalytic activity in a Knoevenagel condensation using benzaldehyde and malononitrile as substrates and toluene as solvent (Scheme 1).[8]

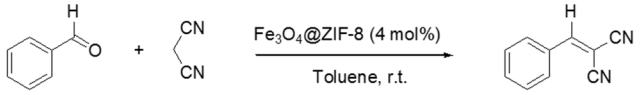


**Scheme 1** $Fe_3O_4$@ZIF-8-catalyzed Knoevenagel reaction between benzaldehyde and malononitrile.

Preliminary experiments showed that the reaction proceeded efficiently at room temperature using 6 equiv. malononitrile relative to benzaldehyde and only 4 mol.% of $Fe_3O_4$@ZIF-8 catalyst, yielding 2-(benzylidene)malononitrile in 94% yield after 3 h of reaction. Under similar experimental conditions, ZIF-8 yielded 2-(benzylidene)malononitrile in 98% yield. Fig. S3 shows the conversion of benzaldehyde when reacting with malononitrile in the presence of ZIF-8 or $Fe_3O_4$@ZIF-8 crystals as a function of time. As seen, the condensations proceeded very quickly at room temperature with both catalysts and the reaction is only slightly slowed down using $Fe_3O_4$@ZIF-8 crystals. These results demonstrate that the iron oxide nanoparticles incorporated in ZIF-8 framework do not alter the activity of ZIF-8 and that the reaction probably proceeds on the external surface of the catalyst. We also conducted a control experiment in which $Fe_3O_4$ nanoparticles were supported on the surface of ZIF-8 crystals by soaking $Fe_3O_4$ particles in an aqueous dispersion of ZIF-8. When benzaldehyde was reacted with malononitrile in the presence of this catalyst, the product of the Knoevenagel condensation was obtained with a yield of 73% after 3 h reaction at room temperature. We believe that the decrease in reactivity in this case may be due to the higher occupation of ZIF-8 catalytically active surface sites. Finally, catalytic cycles were run to investigate the stability of the catalytic activity and recycling. After each run, $Fe_3O_4$@ZIF-8 particles were separated using a magnet, washed twice with toluene and methanol, dried in air at 60°C, and reused. As shown in Fig. S4, the catalyst could be recycled at least ten times without any loss of activity for the Knoevenagel condensation between benzaldehyde and malononitrile.

The loading of magnetite nanoparticles into ZIFs was successfully extended to $Cu^{2+}$-doped ZIF-8 materials developed recently.[44] Citrate-capped $Fe_3O_4$ were successfully immobilized in the $Cu_{25\%}$/ZIF-8 framework and the $Fe_3O_4$@$Cu_{25\%}$/ZIF-8 used for cycloaddition between benzylazide and phenylacetylene (Scheme 2).

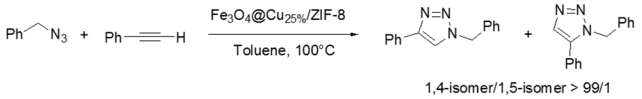


**Scheme 2** Synthesis of 1,2,3-triazoles using $Fe_3O_4$-loaded $Cu^{2+}$-doped ZIF-8 particles.

The triazoles were obtained in 98% isolated yield using a phenylacetylene/benzylazide molar ratio of 1.2 and conducting the reaction for 3 h in toluene at 100°C. Noteworthy is the improvement of regioselectivity of the cycloaddition with $Fe_3O_4$-loaded $Cu_{25\%}$/ZIF-8 as compared to $Cu_{25\%}$/ZIF-8 catalyst (1,4/1,5 > 99/1 for $Fe_3O_4$@$Cu_{25\%}$/ZIF-8 while 1,4/1,5 = 92/8 for $Cu_{25\%}$/ZIF-8). The $Fe_3O_4$@$Cu_{25\%}$/ZIF-8 catalyst could be successfully recycled three times without any loss in activity (Fig. S5). The catalyst activity started to drop in run 4 providing triazoles in ca. 75% yield. A gradual decrease in activity was further observed and triazoles were isolated with ca. 55% yield after the 10th cycle of cycloaddition.

View Article Online
DOI: 10.1039/C5DT01191D



Blank experiments conducted in the presence of citrate-capped $Fe_3O_4$ nanoparticles showed no detectable amounts of Knoevenagel or cycloaddition products and confirmed that both reactions were catalyzed by ZIF-8 materials associated to $Fe_3O_4$. We also examined the leaching behaviour of $Fe_3O_4$@ZIF-8 particles in Knoevenagel and Huisgen reactions. The Fe and Zn contents were determined in the crude reaction products using Inductively Coupled Plasma-Optical Emission Spectrometry (ICP-OES). Low levels for Fe leaching (207 and 39 µg/L in Huisgen and Knoevenagel products, respectively) and Zn leaching (234 and 107 µg/L in Huisgen and Knoevenagel products, respectively) were obtained. These results show that ZIF-8 crystals provide enough binding sites on the surface of $Fe_3O_4$ particles to minimize deterioration and leaching and thus to facilitate efficient catalyst recycling. Finally, the XRD patterns of $Fe_3O_4$@ZIF-8 and $Fe_3O_4$@$Cu_{25\%}$/ZIF-8 catalysts exhibit no significant changes in their crystallinity after five recyclings (Fig. S6), which further confirms their high stability.

## Conclusions

To sum up, we have developed an aqueous-based route for incorporating ca 10 nm-sized $Fe_3O_4$ nanoparticles inside ZIF-8 crystals and used $Fe_3O_4$@ZIF-8 particles as a heterogeneous catalyst for Knoevenagel condensations between benzaldehyde and malononitrile. The $Fe_3O_4$@ZIF-8 catalyst is easily recoverable by magnetic separation and can be reused more than ten times without any loss in the catalytic activity. Using the same approach, $Fe_3O_4$ particles were also loaded into $Cu^{2+}$-doped ZIF-8 crystals and the particles obtained were successfully used for $Cu^{2+}$-catalyzed Huisgen cycloadditions. Results obtained in this study open an avenue to the fabrication of highly efficient and easily recoverable MOFs based nanocatalysts.

## Acknowledgements

This work was supported by ICCEL and MICA Carnot Institutes. We thank Kevin Mozet (LRGP, UMR CNRS 7274, Université de Lorraine) and Hervé Marmier (LIEC, UMR CNRS 7360, Université de Lorraine) for BET and ICP-OES measurements, respectively.

## Notes and references

[a] *Laboratoire Réactions et Génie des Procédés (LRGP), UMR CNRS 7274, Université de Lorraine, 1 rue Grandville 54001 Nancy, France. E-mail: raphael.schneider@univ-lorraine.fr*
[b] *Institut Jean Lamour (IJL), Université de Lorraine, CNRS, UMR 7198, CNRS, BP 70239, 54506 Vandoeuvre-lès-Nancy Cedex, France; Tel: +33 383175053*
[c] *Institut de Science des Matériaux de Mulhouse (IS2M), UMR 7361, CNRS, 15 rue Jean Starcky, 68093 Mulhouse, France*

† Electronic Supplementary Information (ESI) available: Synthetic procedures, size distributions, TEM images of $Fe_3O_4$ nanoparticles, recycling performances of the catalysts, and XRD patterns of materials after catalytic experiments. See DOI: 10.1039/b000000x/

1 R. Morris and P. Wheatley, *Angew. Chem. Int. Ed*., 2008, **47**, 4966-4981.
2 O. K. Farha, A. O. Yazaydin, I. Eryazici, C. D. Malliakas, B. G. Hauser, M. G. Kanatzidis, S. T. Nguyen, R. Q. Snurr and J. T. Hupp, *Nat. Chem*., 2010, **2**, 944-948.
3 J. -R. Li, R. J. Kuppler and H. -C. Zhou, *Chem. Soc. Rev*., 2009, **38**, 1477-1504.
4 B. Chen, C. Liang, J. Yang, D. S. Contreras, Y. L. Clancy, E. B. Lobkovsky, O. M. Yaghi and S. A. Dai, *Angew. Chem. Int. Ed*., 2006, **45**, 1390-1393.
5 K. S. Park, Z. Ni, A. P. Côté, J. Y. Choi, R. D. Huang, F. J. Uribe-Romo, H. K. Chae, M. O'Keeffe and O. M. Yaghi, *Proc. Natl. Acad. Sci. U.S.A*., 2006, **103**, 10186-10191.
6 B. Wang, A. P. Côté, H. Furukawa, M. O'Keeffe and O. M. Yaghi, *Nature*, 2008, **453**, 207-211.
7 R. Banerjee, A. Phan, B. Wang, C. Knobler, H. Furukawa, M. O'Keeffe and O. M. Yaghi, *Science*, 2008, **319**, 939-943.
8 A. Schejn, L. Balan, V. Falk, L. Aranda, G. Medjahdi and R. Schneider, *CrystEngComm*, 2014, **16**, 4493-4500.
9 J. Lee, O. K. Farha, J. Roberts, K. A. Scheidt, S. T. Nguyen and J. T. Hupp, *Chem. Soc. Rev*., 2009, **38**, 1450-1459.
10 D. Guin, B. Baruwati and S. V. Manorama, *Org. Lett*., 2007, **9**, 1419-1421.
11 S. Sun and H. Zeng, *J. Am. Chem. Soc*., 2002, **124**, 8204.
12 A. H. Latham and M. E. Williams, *Acc. Chem. Res*., 2008, **41**, 411-420.
13 S. Laurent, D. Forge, M. Port, A. Roch, C. Robic, L. Vander Elst and R. N. Muller, *Chem. Res*., 2008, **108**, 2064-2110.
14 F. Schröder, D. Esken, M. Cokoja, M. W. E. van den Berg, O. I. Lebedev, G. Van Tendeloo, B. Walaszek, G. Buntkowski, H. -H. Limbach, B. Chaudret and R. A. Fischer, *J. Am. Chem. Soc*., 2008, **130**, 6119-6130.
15 R. J. T. Houk, B. W. Jacobs, F. E. Gabaly, N. N. Chang, A. A. Talin, D. D. Graham, S. D. House, I. M. Robertson and M. D. Allendorf, *Nano Lett*., 2009, **9**, 3413-3418.
16 H. -L. Jiang, B. Liu, T. Akita, M. Haruta, H. Sakurai and Q. Xu, *J. Am. Chem. Soc*., 2009, **131**, 11302-11303.
17 H. Liu, Y. Liu, Y. Li, Z. Tang and H. Jiang, *J. Phys. Chem. C,* 2010, **114**, 13362-13369.
18 M. Meilikhov, K. Yusenko, D. Esken, S. Turner, G. Van Tendeloo and R. A. Fischer, *Eur. J. Inorg. Chem*., 2010, 3701-3714.
19 T. T. Isimjan, H. Kazemian, S. Rohani and A. K. Ray, *J. Mater. Chem.,* 2010, **20**, 10241-10245.
20 H. -L. Jiang and Q. Xu, *Chem. Commun*., 2011, **47**, 3351-3370.
21 K. Sugikawa, Y. Furukawa and K. Sada, *Chem. Mater*., 2011, **23**, 3132-3134.
22 C. Wang, K. E. deKrafft and W. Lin*, J. Am. Chem. Soc*., 2012, **134**, 7211-7214.
23 G. Lu, S. Li, Z. Guo, O.K. Farha, B.G. Hauser, X. Qi, Y. Wang, X. Wang, S. Han, X. Liu, J. S. DuChene, H. Zhang, Q. Zhang, X. Chen, J. Ma, S. C. J. Loo, W. D. Wei, Y. Yang, J. T. Hupp and F. Huo, *Nat. Chem*., 2012, **4**, 310-316.
24 Y. Pan, D. Ma, H. Liu, H. Wu, D. He and Y. Li, *J. Mater. Chem*., 2012, **22**, 10834-10839.
25 Z. Li and H. C. Zeng, *Chem. Mater*., 2013, **25**, 1761-1768.
26 F. Ke, J. Zhu, L. -G. Qiu and X. Jiang, *Chem. Commun*., 2013, **49**, 1267-1269.
27 P. Wang, J. Zhao, X. Li, Y. Yang, Q. Yang and C. Li*, Chem. Commun*., 2013, **49**, 3330-3332.
28 L. Chen, Y. Peng, H. Wang, Z. Gu and C. Duan, *Chem. Commun*., 2014, **50**, 8651-8654.
29 D. Esken, S. Turner, C. Wiktor, S. B. Kalidindi, G. Van Tendeloo and R. A. Fischer, *J. Am. Chem. Soc*., 2011, **133**, 16370-16373.
30 D. Esken H. Noei, Y. Wang, C. Wiktor, S. Turner, G. Van Tendeloo and R. A. Fischer, *J. Mater. Chem*., 2011, **21**, 5907-5915.
31 D. Buso, J. Jasieniak, M. D. H. Lay, P. Schiavuta, P. Scopese, J. Laid, H. Amenitsch, A. J. Hill and P. Falcaro, *Small,* 2012, **8**, 80-88.

View Article Online
DOI: 10.1039/C5DT01191D

32 B. P. Biswal, D. B. Shinde, V. K. Pillai and R. Banerjee, *Nanoscale,* 2013, **5**, 10556-10561.
33 T. Wakaoka, K. Hirai, K. Murayama, Y. Takano, H. Takagi, S. Furukawa and S. Kitagawa, *J. Mater. Chem. C*, 2014, **2**, 7173-7175.
34 Q.-L. Zhu and Q. Xu, *Chem. Soc. Rev.*, 2014, **43**, 5468-5512.
35 S. B. Kim, C. Cai, S. Sun and D. A. Sweigart, *Angew. Chem. Int. Ed.,* 2009, **48**, 2907-2910.
36 Y. Kim, Y.S. Choi, H.J. Lee, H. Yoon, Y.K. Kim and M. Oh, *Chem. Comm*. 2014, **50**, 7617-7620.
37 F. Ke, L. –G. Qiu and J. Zhu, *Nanoscale*, 2014, **6**, 1596-1601.
38 F. Ke, L. Wang and J. Zhu, *Nanoscale* 2015, **7**, 1201-1208.
39 T. Zhang, X. Zhang, X. Yan, L. Kong, G. Zhang, H. Liu, J. Qiu and K. L. Yeung, *Chem. Engineer. J.,* 2013, **228**, 398-404.
40 J Zheng, C. Cheng, W.-J. Fang, C. Chen, R.-W. Yan, H.-X. Huai and C. -C. Wang, *CrystEngComm,* 2014, **16**, 3960-3964.
41 S. R. Ahmed, J. Dong, M. Yui, T. Kato, J. Lee and E. Y. Park, *J. Nanobiotechnol.,* 2013, **11**, 28 (9 pages).
42 F. C. Fonseca, G. F. Goya, R. F. Jardim, R. Mucillo, N. V. L. Carreno, E. Longo and E. R. Leite, *Phys. Rev. B,* 2002, **66**, 104406.
43 S. Morup, F. Bodker, P. V. Hendriksen and S. Linderoth, *Phys. Rev. B,* 1995, **52**, 287.
44 A. Schejn, A. Aboulaich, L. Balan, V. Falk, J. Lalevée, G. Medjahdi, L. Aranda, K. Mozet and R. Schneider, *Catal. Sci. Technol.,* 2015, **5**, 1829-1839.

View Article Online
DOI: 10.1039/C5DT01191D

**Table of contents entry**

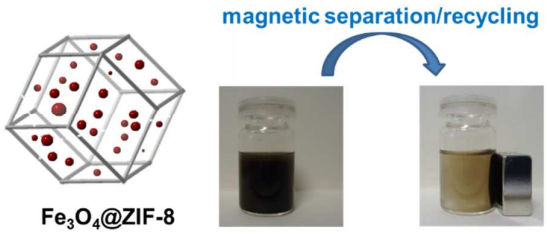


Synthesis and characterization of $Fe_3O_4$ nanoparticles encapsulated in ZIF-8 crystals along with their catalytic properties and reusability are presented.